NATIONAL ADVISORY COMMITTEE FOR AERONAUTICS

REPORT No. 816

COMPARISON OF WIND-TUNNEL AND FLIGHT MEASUREMENTS OF STABILITY AND CONTROL CHARACTERISTICS OF A DOUGLAS A-26 AIRPLANE

By GERALD G. KAYTEN and WILLIAM KOVEN

1945

For sale by the Superintendent of Documents, U. S. Government Printing Office, Washington 25, D. C. - - - - - - - - - Price 15 cents

AERONAUTIC SYMBOLS

1. FUNDAMENTAL AND DERIVED UNITS

	Symbol	Metric		English	
		Unit	Abbreviation	Unit	Abbreviation
Length	l	meter	m	foot (or mile)	ft (or mi)
Time	t	second	s	second (or hour)	sec (or hr)
Force	F	weight of 1 kilogram	kg	weight of 1 pound	lb
Power	P	horsepower (metric)		horsepower	hp
Speed	V	kilometers per hour	kph	miles per hour	mph
		meters per second	mps	feet per second	fps

2. GENERAL SYMBOLS

W Weight$=mg$

g Standard acceleration of gravity$=9.80665$ m/s^2 or 32.1740 ft/sec^2

m Mass$=\frac{W}{g}$

I Moment of inertia$=mk^2$. (Indicate axis of radius of gyration k by proper subscript.)

μ Coefficient of viscosity

ν Kinematic viscosity

ρ Density (mass per unit volume)

Standard density of dry air, 0.12497 kg-m^{-4}-s^2 at 15° C and 760 mm; or 0.002378 lb-ft^{-4} sec^2

Specific weight of "standard" air, 1.2255 kg/m^3 or 0.07651 lb/cu ft

3. AERODYNAMIC SYMBOLS

S Area

S_w Area of wing

G Gap

b Span

c Chord

A Aspect ratio, $\frac{b^2}{S}$

V True air speed

q Dynamic pressure, $\frac{1}{2}\rho V^2$

L Lift, absolute coefficient $C_L=\frac{L}{qS}$

D Drag, absolute coefficient $C_D=\frac{D}{qS}$

D_0 Profile drag, absolute coefficient $C_{D_0}=\frac{D_0}{qS}$

D_i Induced drag, absolute coefficient $C_{D_i}=\frac{D_i}{qS}$

D_p Parasite drag, absolute coefficient $C_{Dp}=\frac{D_p}{qS}$

C Cross-wind force, absolute coefficient $C_C=\frac{C}{qS}$

i_w Angle of setting of wings (relative to thrust line)

i_t Angle of stabilizer setting (relative to thrust line)

Q Resultant moment

Ω Resultant angular velocity

R Reynolds number, $\rho\frac{Vl}{\mu}$ where l is a linear dimension (e.g., for an airfoil of 1.0 ft chord, 100 mph, standard pressure at 15° C, the corresponding Reynolds number is 935,400; or for an airfoil of 1.0 m chord, 100 mps, the corresponding Reynolds number is 6,865,000)

α Angle of attack

ϵ Angle of downwash

α_o Angle of attack, infinite aspect ratio

α_i Angle of attack, induced

α_a Angle of attack, absolute (measured from zero-lift position)

γ Flight-path angle

REPORT No. 816

COMPARISON OF WIND-TUNNEL AND FLIGHT MEASUREMENTS OF STABILITY AND CONTROL CHARACTERISTICS OF A DOUGLAS A–26 AIRPLANE

By GERALD G. KAYTEN and WILLIAM KOVEN

Langley Memorial Aeronautical Laboratory
Langley Field, Va.

National Advisory Committee for Aeronautics

Headquarters, 1500 New Hampshire Avenue NW., Washington 25, D. C.

Created by act of Congress approved March 3, 1915, for the supervision and direction of the scientific study of the problems of flight (U. S. Code, title 49, sec. 241). Its membership was increased to 15 by act approved March 2, 1929. The members are appointed by the President, and serve as such without compensation.

TECHNICAL COMMITTEES

AERODYNAMICS

POWER PLANTS FOR AIRCRAFT

AIRCRAFT CONSTRUCTION

OPERATING PROBLEMS

MATERIALS RESEARCH COORDINATION

Coordination of Research Needs of Military and Civil Aviation

Preparation of Research Programs

Allocation of Problems

Prevention of Duplication

LANGLEY MEMORIAL AERONAUTICAL LABORATORY
Langley Field, Va.

AMES AERONAUTICAL LABORATORY
Moffett Field, Calif.

AIRCRAFT ENGINE RESEARCH LABORATORY, Cleveland Airport, Cleveland, Ohio

Conduct, under unified control, for all agencies, of scientific research on the fundamental problems of flight

---

OFFICE OF AERONAUTICAL INTELLIGENCE, Washington, D. C.

Collection, classification, compilation, and dissemination of scientific and technical information on aeronautics

REPORT No. 816

COMPARISON OF WIND-TUNNEL AND FLIGHT MEASUREMENTS OF STABILITY AND CONTROL CHARACTERISTICS OF A DOUGLAS A–26 AIRPLANE

By Gerald G. Kayten and William Koven

SUMMARY

Stability and control characteristics determined from tests in the Langley 19-foot pressure tunnel of a 0.2375-scale model of the Douglas XA–26 airplane are compared with those measured in flight tests of a Douglas A–26B airplane.

Agreement regarding static longitudinal stability as indicated by the elevator-fixed neutral points and by the variation of elevator deflection in both straight and turning flight was found to be good except at speeds approaching the stall. At these low speeds the airplane possessed noticeably improved stability, which was attributed to pronounced stalling at the root of the production wing. The pronounced root stalling did not occur on the smooth, well-faired model wing. Elevator tab effectiveness determined from model tests agreed well with flight-test tab effectiveness, but control-force variations with speed and acceleration were not in good agreement. Although some discrepancy was introduced by the absence of a seal on the model elevator and by small differences in the determination of elevator deflections, correlation in control-force characteristics was also influenced by the effects of fabric distortion at high speeds and by small construction dissimilarities such as differences in trailing-edge angle. Except for the wave-off condition, in which the tunnel results indicated rudder-force reversal at a higher speed than the flight tests, agreement in both rudder-fixed and rudder-free static directional stability was good. Model and airplane indications of stick-fixed and stick-free dihedral effect were also in good agreement, although some difference in geometric dihedral may have existed because of wing bending in flight. The use of model hinge-moment data obtained at zero sideslip appeared to be satisfactory for the determination of aileron forces in sideslip. Fairly good correlation in aileron effectiveness and control forces was obtained; fabric distortion may have been responsible to some extent for higher flight values of aileron force at high speeds. Estimation of sideslip developed in an abrupt aileron roll was fair, but determination of the rudder deflection required to maintain zero sideslip in a rapid aileron roll was not entirely satisfactory.

INTRODUCTION

Although the qualitative reliability of wind-tunnel stability and control test results is generally accepted, very few opportunities have arisen for determination of the quantitative agreement between measured flying qualities of an airplane and flying qualities predicted on the basis of model tests.

In connection with the development of the Douglas A–26 twin-engine attack bomber, a series of investigations has been conducted at the Langley Laboratory of the National Advisory Committee for Aeronautics. These investigations, the results of which have not been published, included tests of a 0.2375-scale powered model of the XA–26 airplane in the Langley 19-foot pressure tunnel and flight tests of an A–26B airplane. By use of the unpublished wind-tunnel data, calculations have been made predicting the flying qualities of the airplane for correlation with the characteristics measured in the flight tests. The results of the correlation are presented herein; the flying qualities are not discussed except for the purpose of comparison.

MODEL, AIRPLANE, AND TESTS

Photographs and drawings of the A–26B airplane and the XA–26 model are shown as figures 1 and 2, respectively.

(a) A–26B airplane.

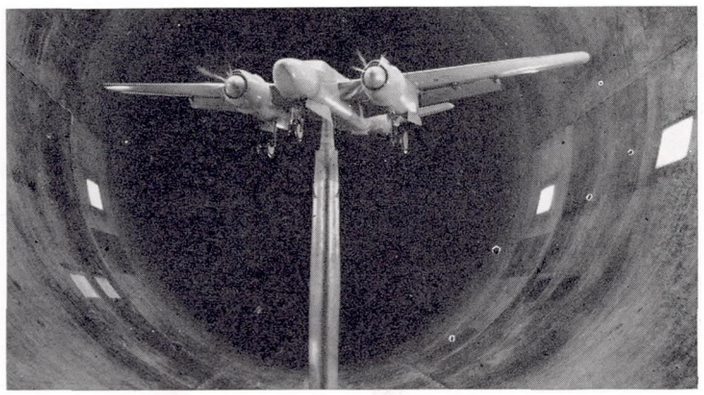

(b) 0.2375-scale model of XA–26 airplane mounted in Langley 19-foot pressure tunnel.

Figure 1.—Three-quarter front views of Douglas A–26 airplane and model.

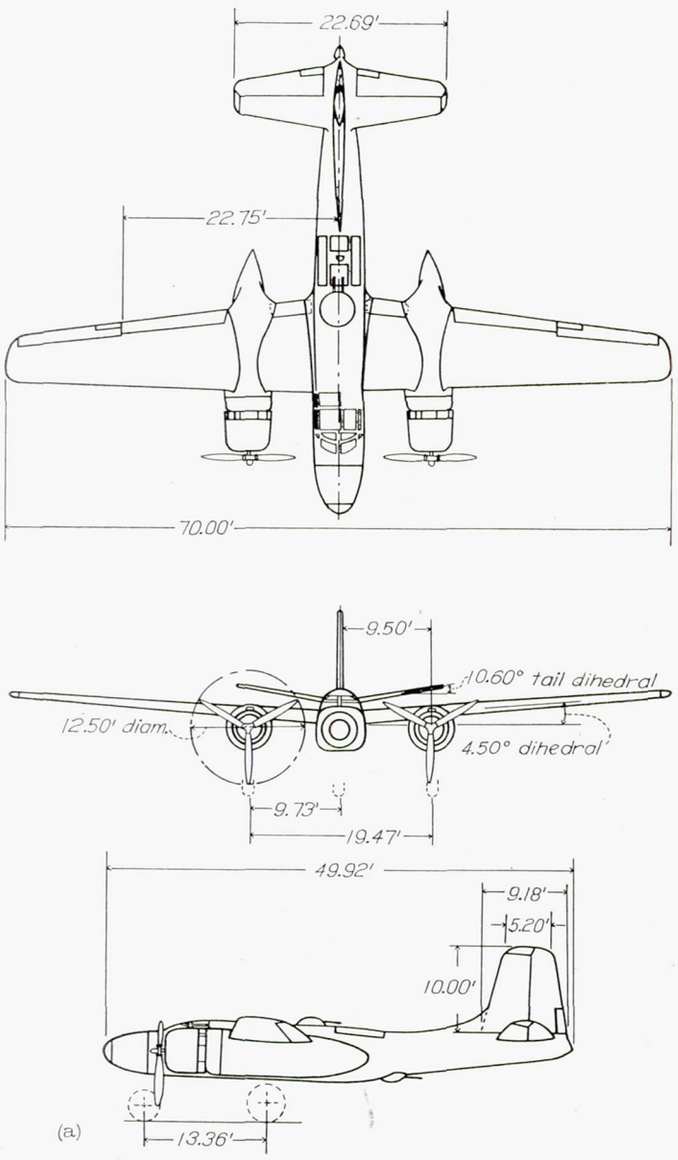

(a) A–26B airplane.

FIGURE 2.—Three-view drawings of a Douglas A–26 airplane and model.

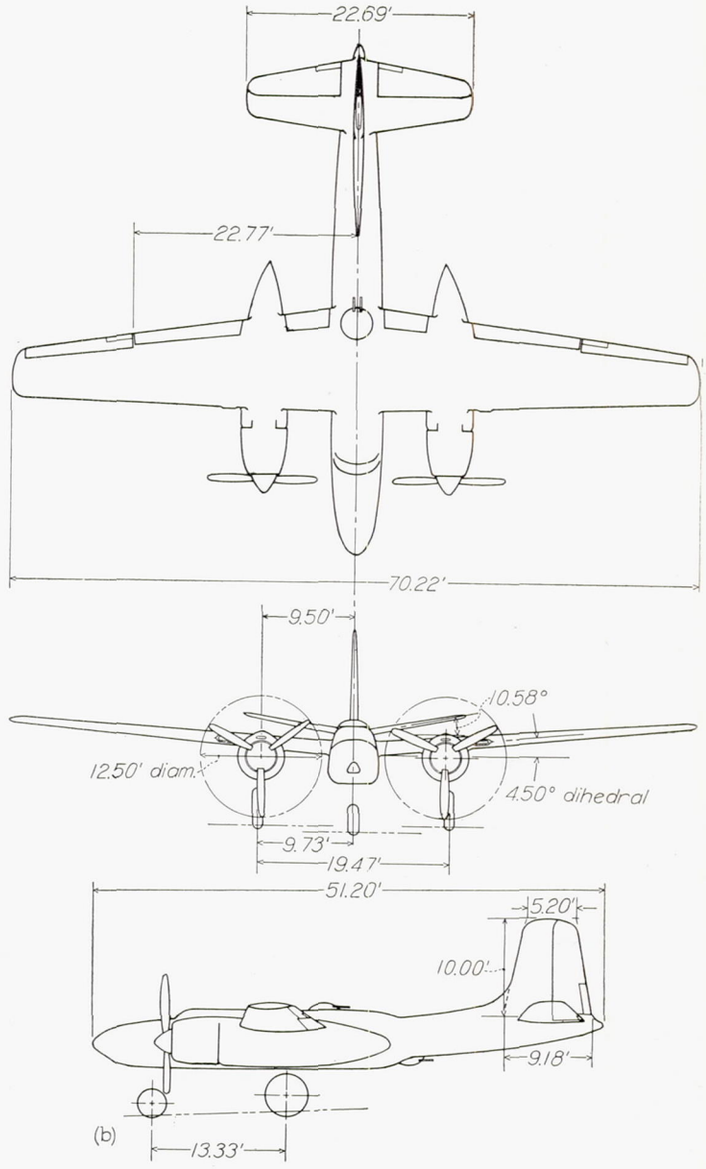

(b) 0.2375-scale model of Douglas XA–26 airplane. (Dimensions are those of the 0.2375-scale model converted to airplane size.)

FIGURE 2.—Concluded.

In table I general dimensions and specifications are shown for the airplane and the model, as well as for the model scaled up to airplane size. Some discrepancies of negligible importance are noted in this table but it can be seen that, with respect to general dimensions, the XA–26 and the A–26B are essentially the same airplane. As shown in figure 1, the model during the stability and control tests was equipped with a fuselage nose which was somewhat different from that of the airplane. The spinners shown on the model propellers were not used on the airplane, and the airplane oil-cooler ducts outboard of the nacelles were removed from the model wing during the stability and control tests with the exception of the aileron tests.

Several more significant differences existed between the model and the airplane. During most of the tunnel tests the model rudder and the elevator, which were of the plain overhang-balance type, remained unsealed, but the airplane control surfaces were equipped with rubberized canvas seals. The control surfaces, all of which were fabric-covered on the airplane, were of rigid metal construction on the model. The airplane ailerons were equipped with balancing tabs arranged so that 8° of aileron deflection produced approximately 3° of opposite tab deflection. On the model the balancing tab when connected moved 1° for a 1° aileron deflection.

TABLE I—GENERAL DIMENSIONS AND SPECIFICATIONS

Item	0.2375–scale XA–26 model	Full scale based on 0.2375-scale model	Full-scale A–26B
Wing:			
Area, sq ft	30.488	540.510	540.0
Span, ft	16.676	70.22	70.0
M. A. C., ft	1.930	8.13	8.13
Geometric aspect ratio	9.08	9.08	9.07
Taper ratio	0.453	0.453	0.45
Sweepback of L.E., deg	1.90	1.90	1.90
Incidence, root, deg	2	2	2
Incidence, tip, deg	1	1	1
Dihedral, deg	4.5	4.5	4.5
Airfoil section, root	NACA 65(216)–215 (a=0.8, b=1.0)	NACA 65(216)–215 (a=0.8, b=1.0)	NACA 65(216)–215 (a=0.8, b=1.0)
Airfoil section, tip	NACA 65(216)–215 (a=0.5, b=1.0)	NACA 65(216)–215 (a=0.5, b=1.0)	NACA 65(216)–215 (a=0.5, b=1.0)
Wing flaps (double slotted):			
Area (behind hinge line), sq ft	3.154	55.91	55.9
Ailerons:			
Area (behind hinge line, total of two ailerons including tabs), sq ft	1.536	27.23	27.2
Span, ft	2.59	10.92	11.0
Balance-tab area, total, sq ft	0.134	2.38	2.3
Horizontal tail:			
Span, ft	5.387	22.69	22.69
Area, including fuselage, sq ft	6.549	116.10	116.10
Incidence, deg	0	0	0
Dihedral, deg	10.58	10.58	10.60
Elevator area (behind hinge line), sq ft	1.842	32.66	32.7
Balance area, sq ft	0.581	10.30	10.3
Trimming-tab area, total, sq ft	0.146	2.58	2.6
Distance elevator hinge line to 25 percent M. A. C. of wing, ft	7.127	30.06	30.05
Vertical tail:			
Area (excluding dorsal), sq ft	4.03	71.35	71.35
Rudder area (behind hinge line), sq ft	1.30	23.12	23.1
Trimming-tab area, sq ft	0.13	2.28	2.28
Height above top of fuselage, ft	2.375	10.00	10.0
Propeller:			
Diameter, ft	2.97	12.50	12.50

Thin metal strips were fastened to the upper and lower surfaces of the airplane elevator causing small ridges directly in front of the tab. These ridges were not represented on the model, but their effect on elevator and tab characteristics is believed to be negligible.

The wind-tunnel program included a fairly extensive series of conventional stability and control tests. The model aileron tests were made at a Reynolds number of approximately 5.4×10^6. The remaining model tests were made at a Reynolds number of approximately 3.6×10^6 except for the tests at high thrust coefficients, which because of model motor limitations were made at Reynolds numbers reduced to approximately 2.6×10^6. The portion of the flight tests devoted to stability and control were of the type usually conducted by the NACA for the purpose of determining the flying qualities of an airplane. The weight of the airplane, which varied from 27,000 to 31,000 pounds in the flight tests, was assumed for the analysis of the tunnel data to be 28,000 pounds corresponding to a wing loading of 51.8 pounds per square foot. The analysis was based on an altitude of 10,000 feet, which represented an approximate mean of the flight-test altitudes.

Analysis of the tunnel data has been made for conditions representing airplane rated power and 75-percent rated power at the appropriate airplane weight and altitudes and for a gliding flight condition. In representation of the gliding flight condition, it has been assumed that engines-idling and zero-thrust conditions may be considered identical. Any discrepancy in results introduced by the difference between these power conditions probably will be small.

In computing elevator, aileron, and rudder control forces from model hinge-moment data, the corresponding control linkages measured on the airplane were used.

COEFFICIENTS AND SYMBOLS

δ_e elevator deflection, degrees
δ_f flap deflection, degrees
δ_t tab deflection, degrees
C_h hinge-moment coefficient $\left(\frac{H}{q b_e \bar{c}^2}\right)$
V_i indicated airspeed, miles per hour
F_e elevator control force, pounds
T_c thrust coefficient $\left(\frac{T}{\rho V^2 D^2}\right)$
$\frac{pb}{2V}$ wing-tip helix angle, radians
C_L lift coefficient $\left(\frac{\text{Lift}}{qS}\right)$

where

H hinge moment, foot-pounds
b_e span of control surface, feet
$\bar{c}$ root-mean-square chord, feet
q dynamic pressure, pounds per square foot $\left(\frac{1}{2}\rho V^2\right)$
ρ mass density of air, slugs per cubic foot
V airspeed, feet per second
T total thrust (two propellers), pounds
D propeller diameter, feet
p rolling velocity, radians per second
b wing span, feet
S wing area, square feet
α angle of attack, degrees
α_t tail angle of attack, degrees
g acceleration of gravity, feet per second per second

RESULTS AND DISCUSSION

LONGITUDINAL STABILITY AND CONTROL

Curves of elevator angle and elevator control force required for trim in straight flight throughout the speed range are shown in figure 3. Various flap and power combinations are considered at three center-of-gravity locations. For the flaps-retracted conditions, the tunnel control-force curves were obtained by applying the tab-effectiveness data of figure 4 to the tab-neutral curves estimated from the tunnel hinge-moment data. The amount of tab deflection required to adjust the tunnel curve for trim at the flight-test trim speed was determined for each power condition and center-of-gravity location, and this amount of tab deflection was assumed constant throughout the speed range. Inasmuch as model trim-tab tests were not made with flaps deflected, the trimmed control-force curves for this condition were obtained by means of a constant adjustment to each original curve of C_h against C_L. This constant hinge-moment shift is believed justified because the data of figure 4 indicate a negligible change in tab effectiveness with change in power (flaps retracted) and because analysis of stabilizer-effectiveness data indicates that the variation in average dynamic-pressure ratio with speed is small for the flaps-deflected condition. The flaps-deflected control-force curves for zero trim tab are included in figure 3.

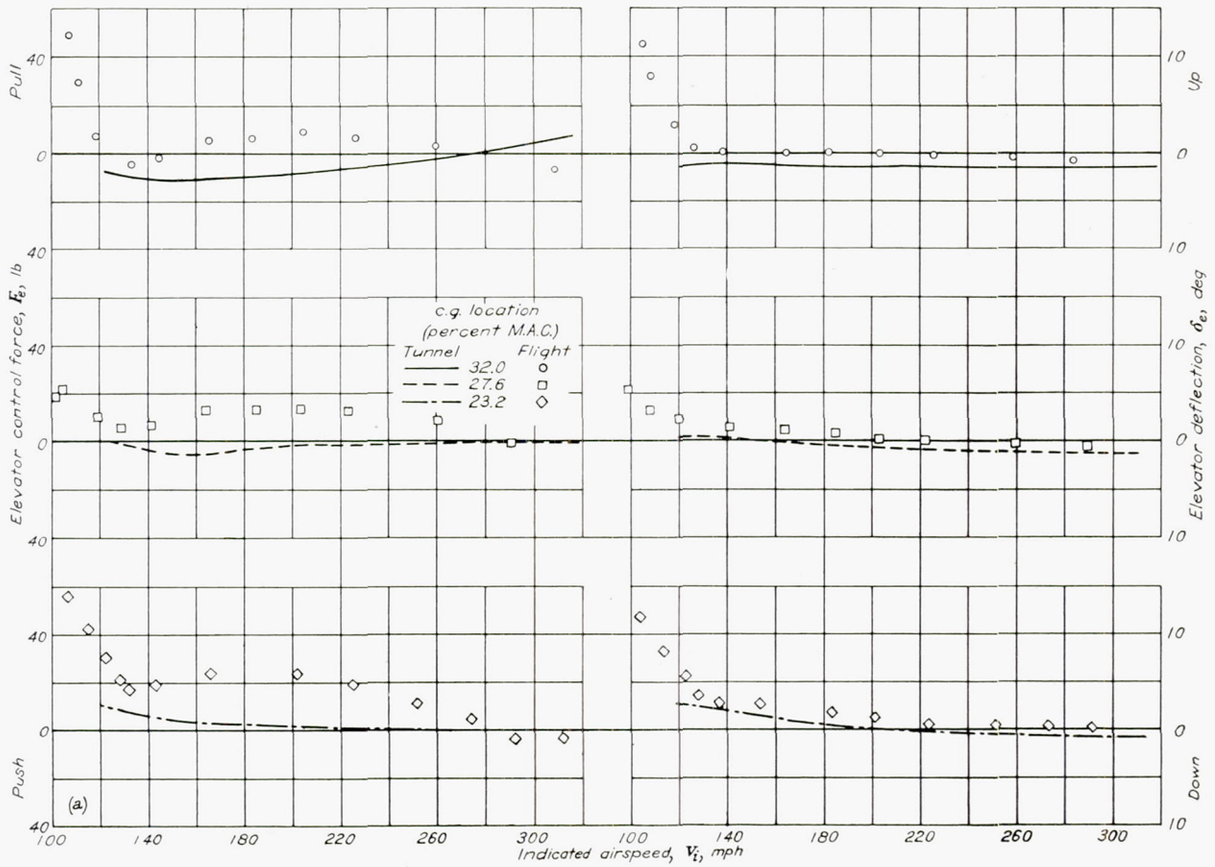

(a) Flaps retracted; rated power.

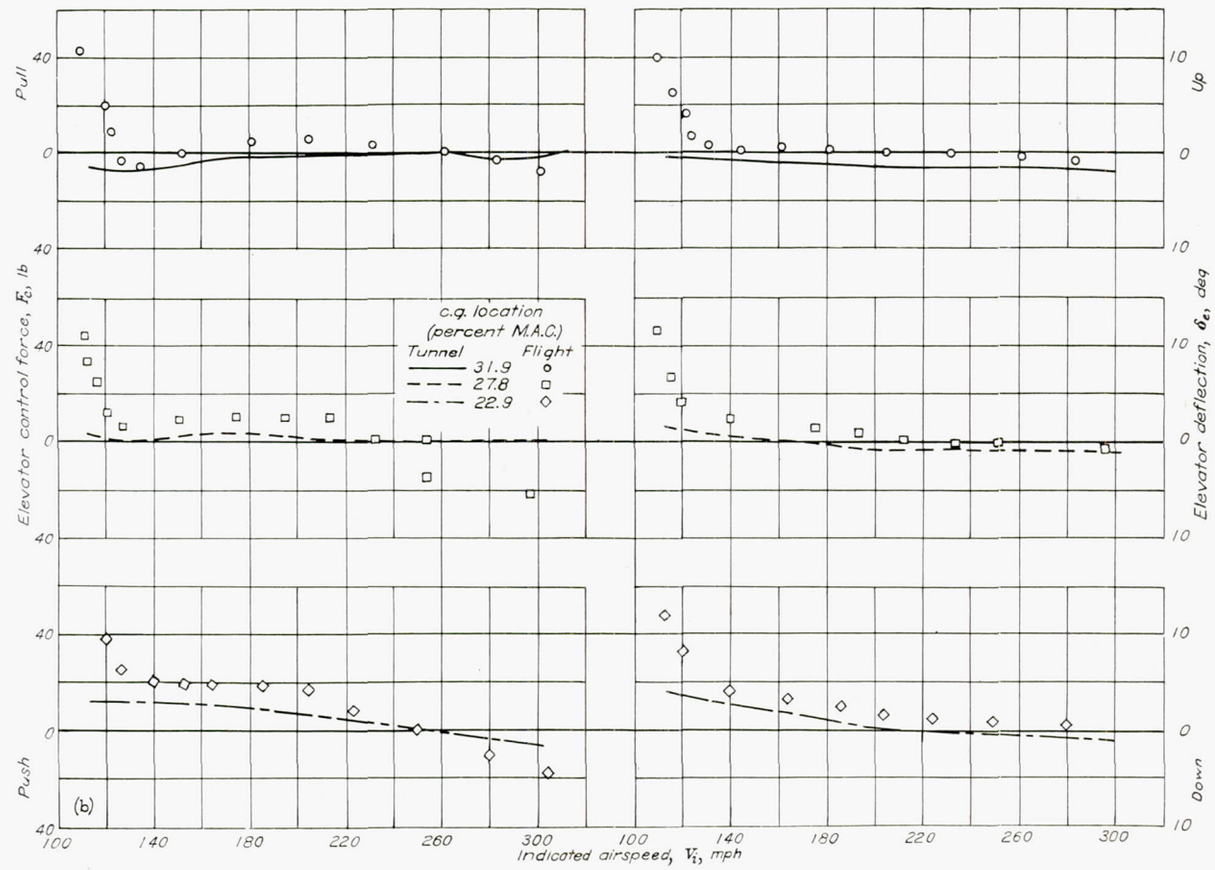

(b) Flaps retracted; 75-percent rated power.

FIGURE 3.—Variation of elevator deflection and control force with indicated airspeed.

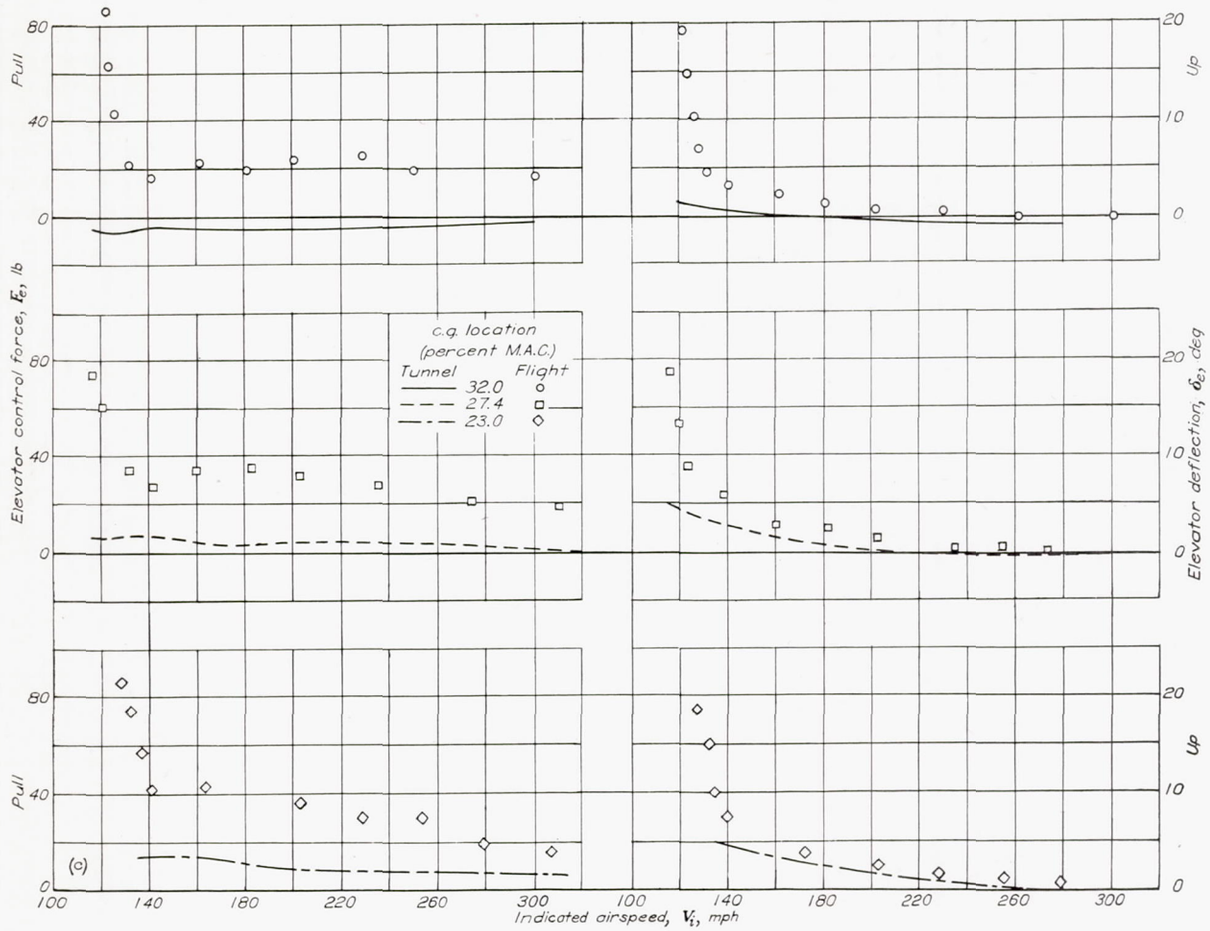

(c) Flaps retracted; $T_c=0$.

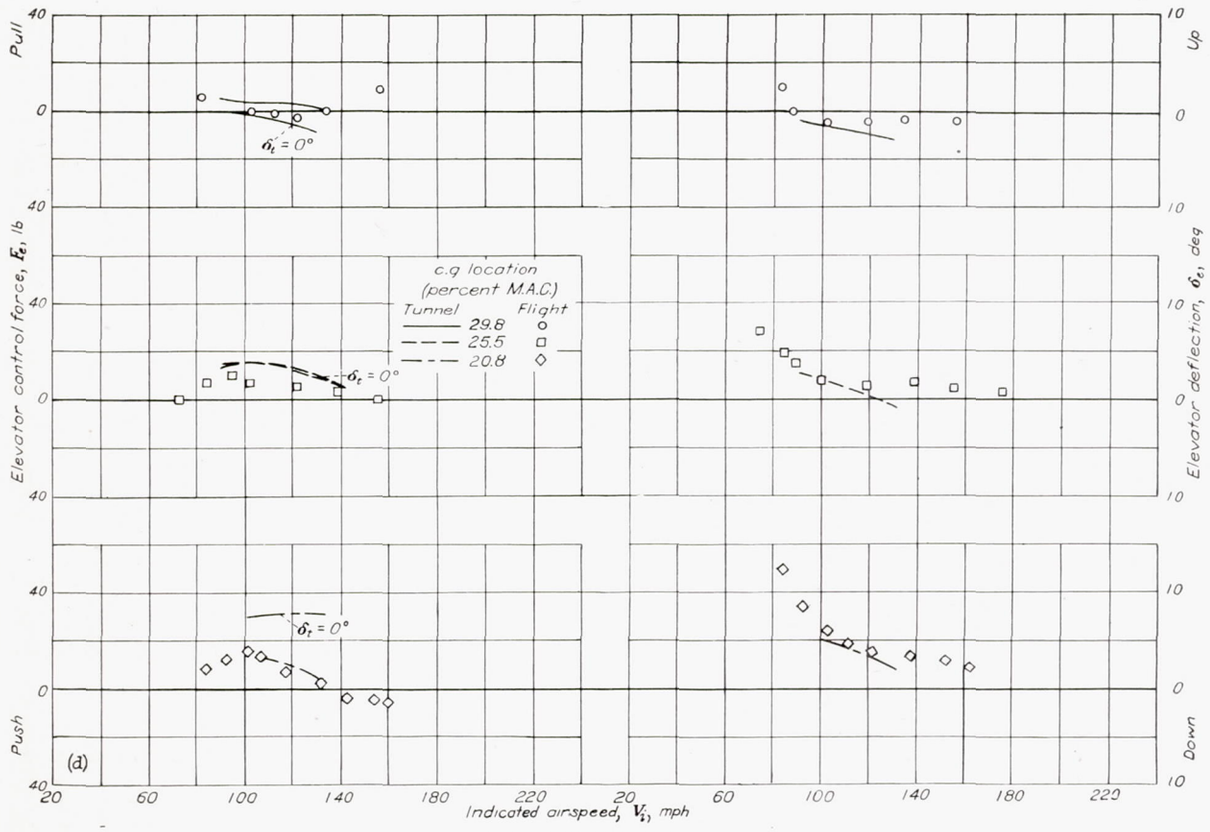

(d) Flaps deflected; rated power.

FIGURE 3.—Concluded.

The sideslip required for straight flight at low speeds was considered to have a negligible effect on the longitudinal characteristics of this airplane; hence, the characteristics determined from tunnel data are based on tests at zero sideslip.

The variation of tab effectiveness with speed has been calculated from flaps-retracted wind-tunnel tests made at elevator-tab settings of 3° and −3° with $\delta_e=0°$ and is shown in figure 4 compared with the flight-test curve.

Elevator deflections and control forces in steady turning flight are shown in figures 5 to 7 for various center-of-gravity locations. The calculated results are based on tunnel tests at the thrust coefficient approximately corresponding to the appropriate flight-test conditions.

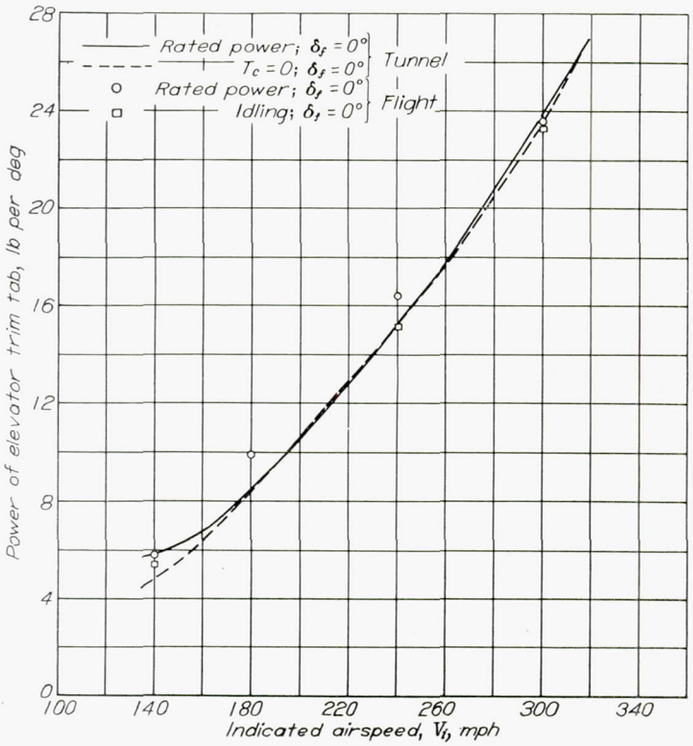

FIGURE 4.—Variation of elevator trim-tab effectiveness with airspeed.

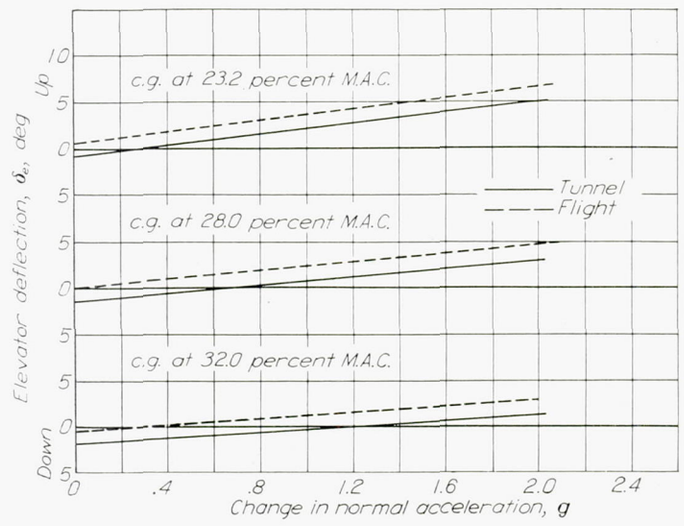

FIGURE 5.—Variation of elevator deflection with normal acceleration in steady turns. V_i=260 miles per hour at 10,000-foot altitude; δ_f=0°; rated power.

Although some small differences exist in the absolute elevator angles, the slopes of the curves in figures 3, 5, and 7 show good agreement between tunnel and flight results for both straight and turning flight, except at speeds close to the stall. At these low speeds, the flight data show pronounced increases in the amount of up-elevator movement required for speed reduction in straight flight. These marked increases

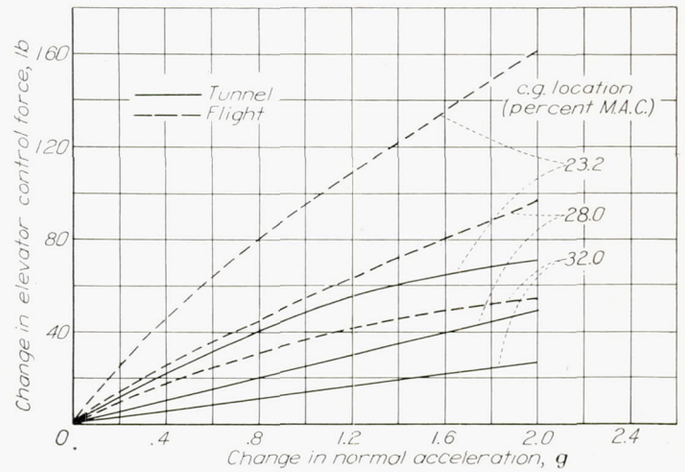

FIGURE 6.—Variation of elevator control force with normal acceleration in steady turns. V_i=260 miles per hour at 10,000-foot altitude; δ_f=0°; rated power.

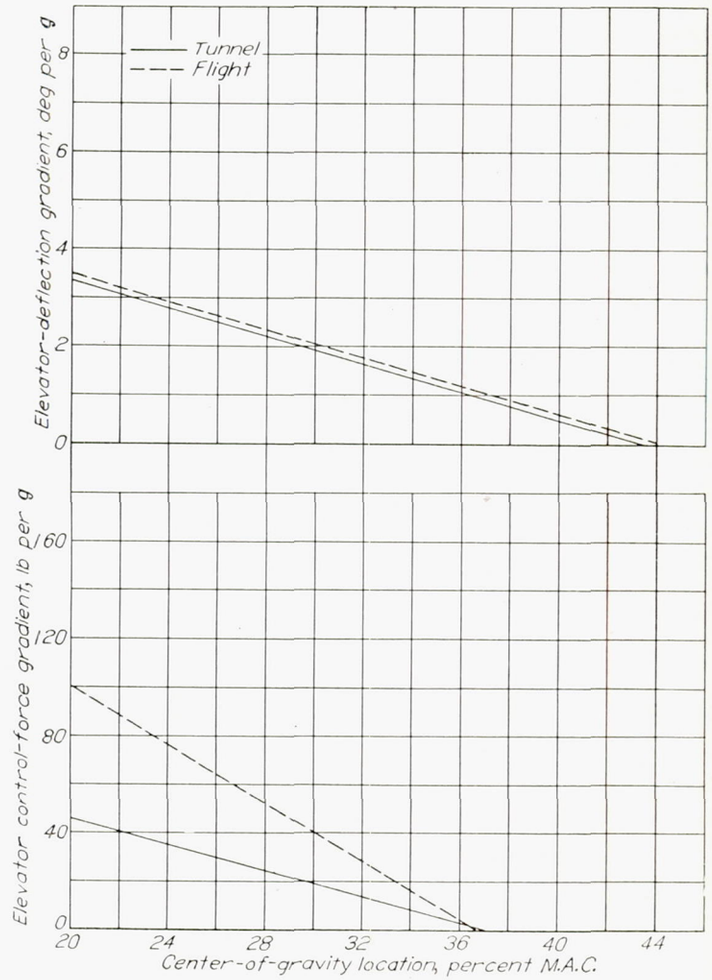

FIGURE 7.—Variation of elevator control-force and deflection gradients with center-of-gravity location. V_i=260 miles per hour at 10,000-foot altitude; δ_f=0°; rated power; steady turning flight

are not apparent in the tunnel data. This discrepancy in results is believed due largely to the fact that the production airplane exhibited a decidedly more definite stall at the wing root than did the smooth, polished model. Although direct comparison of identical configurations is not possible, the difference in stalling characteristics at the wing root is indicated by the diagrams of tunnel and flight-test tuft studies shown in figures 8 and 9. The more pronounced root stalling on the airplane would, in all probability, be accompanied by a reduction in downwash and rate of downwash at the horizontal tail as well as a decrease in wing pitching moment, resulting in an improvement in stability and requiring greater up-elevator deflections for trim. At higher airspeeds the agreement between flight and tunnel results is reasonably consistent with the experimental accuracy of both.

The tunnel and flight curves of elevator-fixed neutral point plotted against airspeed in figure 10 for the flaps-neutral conditions agree to within approximately 2 percent of the mean aerodynamic chord except at low speeds with idling power. This difference is practically within the bounds of the experimental accuracy with which the flight and the wind-tunnel neutral points are determined. The discrepancy increases with reduced airspeed as the airplane demonstrates comparatively greater stability. Because of the difficulty in obtaining consistent neutral-point results, particularly at very high airspeeds, neutral points were not determined for high speeds. The curves of figure 3 serve as a measure of the stability in the high-speed range and are, in fact, believed more reliable for comparison throughout the speed range than the neutral-point curves. Although the curves for the flaps-deflected conditions are included for completeness, direct comparison should not be made inasmuch as the flap settings used in flight and tunnel tests are not identical.

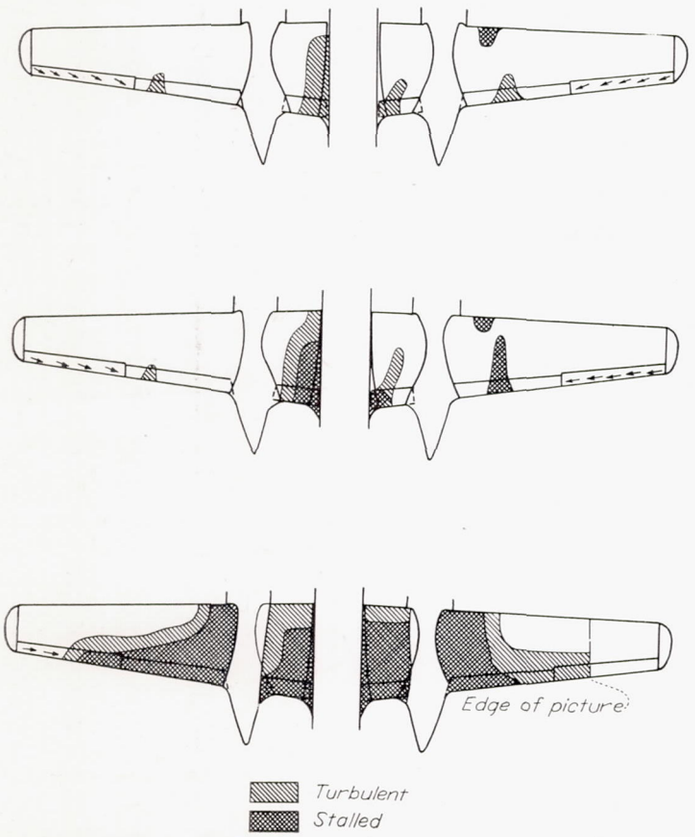

FIGURE 8.—Diagrams of stall progression in the gliding condition. Engines idling; flaps and landing gear up; cowl flaps closed; oil cooler one-half open; Douglas A–26B airplane.

Examination of the straight-flight control-force curves of figure 3 reveals comparatively poor agreement between tunnel and flight results. The force measurements shown in the tab-effectiveness curves of figure 4, however, are in excellent agreement. Both flight and tunnel control-force measurements are believed to be accurate to within approximately ± 3 pounds. Although some discrepancy in the elevator-control-force curves of figure 3 would be expected because of the absence of a seal on the model elevator, analysis based on brief check tests in which the model elevator was sealed indicated that differences of the magnitude shown in figure 3 cannot be attributed to effects of the elevator seal. In an effort to determine the cause of the disagreement, the effects of the discrepancies in elevator deflection were investigated. Hypothetical control forces were computed from tunnel hinge-moment data by using the values of elevator deflection determined from flight rather than those determined from tunnel data. For these computations, the wind-tunnel tab-effectiveness data were used, but the tab deflection was that employed in the flight tests. The curves obtained in this manner are shown in figure 11 compared with the flight-test data. In general, agreement in figure 11 appears considerably improved; for several flight conditions, in fact, agreement is excellent up to speeds above 200 miles per hour, beyond which the flight-test curves become noticeably more stable. This difference may be explained to some extent by the observations of elevator-fabric distortion and internal pressures made during the flight tests. The internal pressures were found to be only slightly higher than free-stream static pressure, causing fabric distortion of the type illustrated in figure 12. As demonstrated in reference 1, elevator-fabric distortion of this type may be expected to produce increases in the variation of force with airspeed at high speeds. Inasmuch as the flaps-retracted flight-test trim speeds of figure 3 are all in this high-speed range, the trim-tab deflections required to trim the control forces computed from tunnel data are different from the tab angles used in flight; and the control forces originally computed from tunnel data (by using the amount of tab deflection required for zero force at the high-speed-flight trim point) could not be expected to agree well with the flight control forces. The lack of agreement in the original results was further aggravated by the elevator-deflection differences at low speeds, caused by the root stalling effects.

In addition to the effects of elevator-deflection differences, fabric distortion, and elevator gap, agreement in the control-force results is believed to be influenced by small but significant construction discrepancies as, for example, differences in surface condition and in trailing-edge angle. At a representative section the trailing-edge angle measured on the model elevator was 12.7°, whereas the corresponding angle measured on the airplane was 11°. None of these effects would be expected to influence appreciably the agreement in tab-effectiveness results.

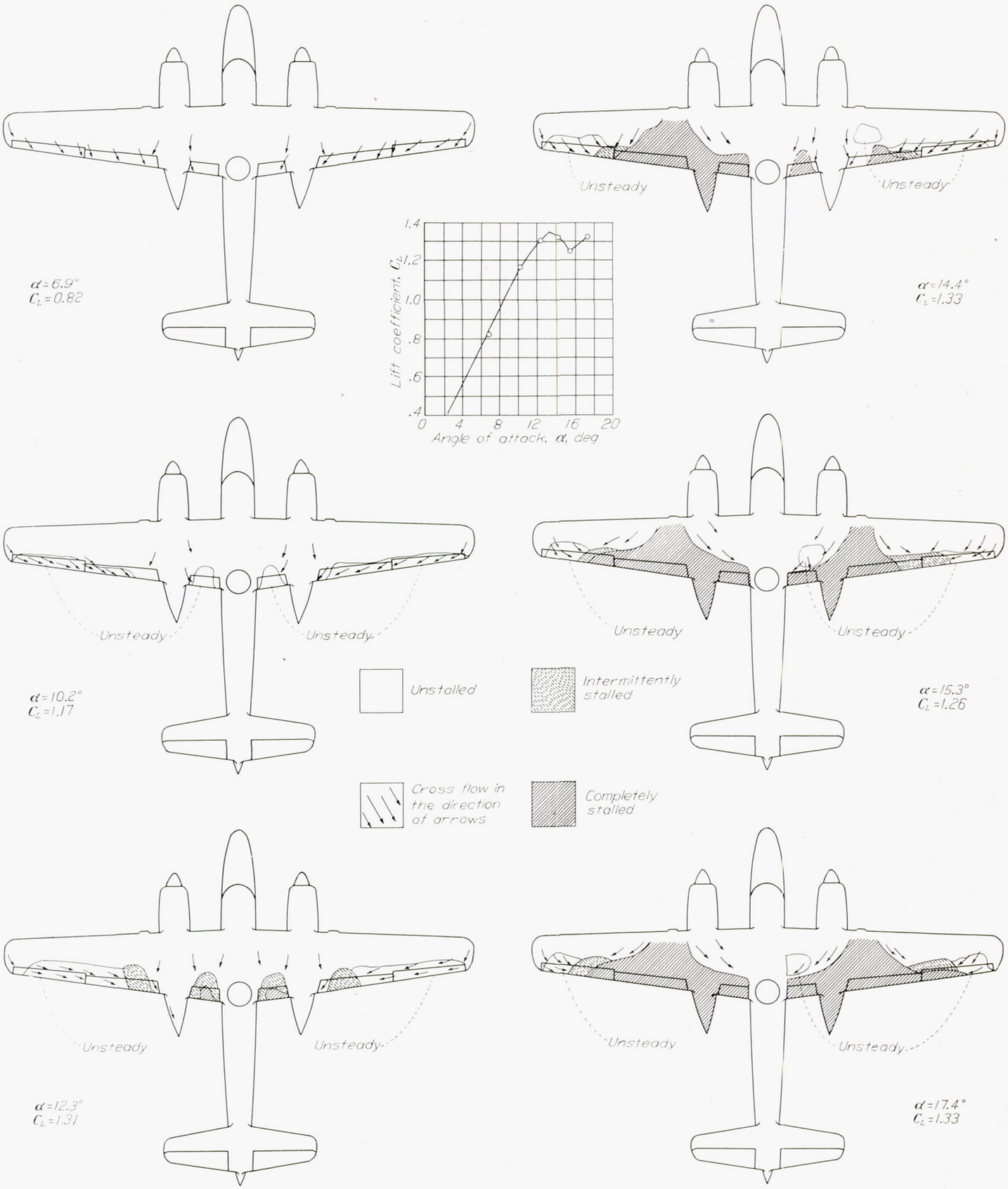

FIGURE 9.—Power-off stall diagrams for the 0.2375-scale model of the XA-26 airplane. Standard model configuration with airplane oil-cooler ducts; Reynolds number, 4.25×10^6; Mach number, 0.131; $\delta_f = 0°$.

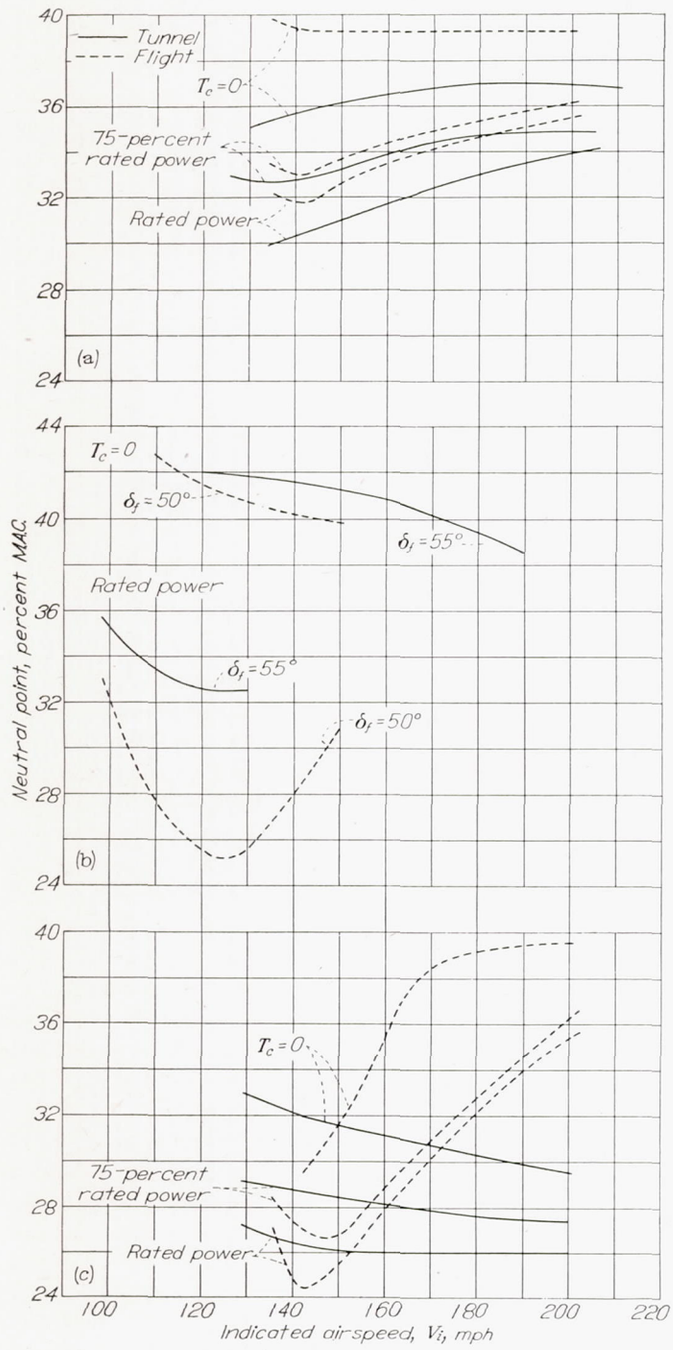

(a) Elevator fixed; flaps neutral.

(b) Elevator fixed; flaps deflected.

(c) Elevator free; flaps neutral.

FIGURE 10.—Variation of neutral point with airspeed in straight flight.

As seen in figures 6 and 7, the flight tests show considerably greater variations of control force with acceleration, and the values of force per g show considerably greater variation with center-of-gravity location, although the elevator-free maneuver point $\frac{F_e}{g}=0$ is approximately the same. Because the absence of an elevator seal was believed to be more significant in accelerated flight than in straight flight, control forces were estimated for both the sealed and the unsealed elevators by assuming constant pitching-moment and hinge-moment slopes and using the sealed-elevator hinge-moment data obtained in the previously mentioned check tests. The respective values of $\partial C_h/\partial\delta_e$ and $\partial C_h/\partial\alpha_t$ used in these computations were -0.0037 and -0.0018 for the unsealed elevator and -0.0050 and -0.0032 for the sealed elevator. The resulting curves of force per g against center-of-gravity location are shown in figure 13. The curve for the unsealed elevator is practically identical with that previously determined for the unsealed elevator (fig. 7) by the method of reference 2. For the sealed elevator the values of force per g are still very much lower than the flight-test values, although the variation of F_e/g with center-of-gravity location is more nearly parallel to that determined in flight. The comparison of control forces in accelerated flight has been made at a fairly high speed. Reference 1 indicates that fabric distortion of the type experienced in the A–26B flight tests may be expected to produce increases in the variation of force with acceleration in the normal center-of-gravity range and in the variation of force per g with center-of-gravity location. This comparison as well as that for straight flight would also be influenced by any differences in control-surface construction.

Agreement in the curves of elevator-free neutral point against airspeed (fig. 10 (c)) is rather poor and becomes worse as the speed increases. The flight-test elevator-free neutral point moves rapidly rearward with increasing speed, and at high speeds the airplane appears more stable with elevator free than with elevator fixed. It is believed that this large rearward shift in the elevator-free neutral point with increasing airspeed may be a result of the fabric distortion.

In general, the present correlation indicates that successful prediction of elevator control-force characteristics from wind-tunnel data can be made only if extreme care is used in representing closely the airplane in its construction form—particularly with regard to the control surfaces. Agreement with flight measurements might also be improved considerably if effects such as fabric distortion could be taken into account. A more beneficial solution, however, would be to minimize these effects in the construction of the airplane.

LATERAL STABILITY AND CONTROL

Steady-sideslip characteristics.—Characteristics of the airplane in steady sideslips, which are used as flight-test measures of directional stability, directional control, dihedral effect, side-force characteristics, and pitching moment due to sideslip, are shown in figure 14. Although complete hinge-moment data for the model ailerons and elevator were not obtained in sideslip, aileron forces in sideslip were estimated from the tunnel data by taking into account the change in effective angle of attack due to sideslip but assuming no direct change in aileron hinge-moment characteristics with sideslip.

For both idling and rated-power flight with flaps retracted, figure 14 shows excellent agreement in the variation of control settings, angle of bank, and rudder force with sideslip, although some difference exists in absolute values. Some of the difference in absolute values may be due to the fact that model tare tests were not made in sideslip. It is

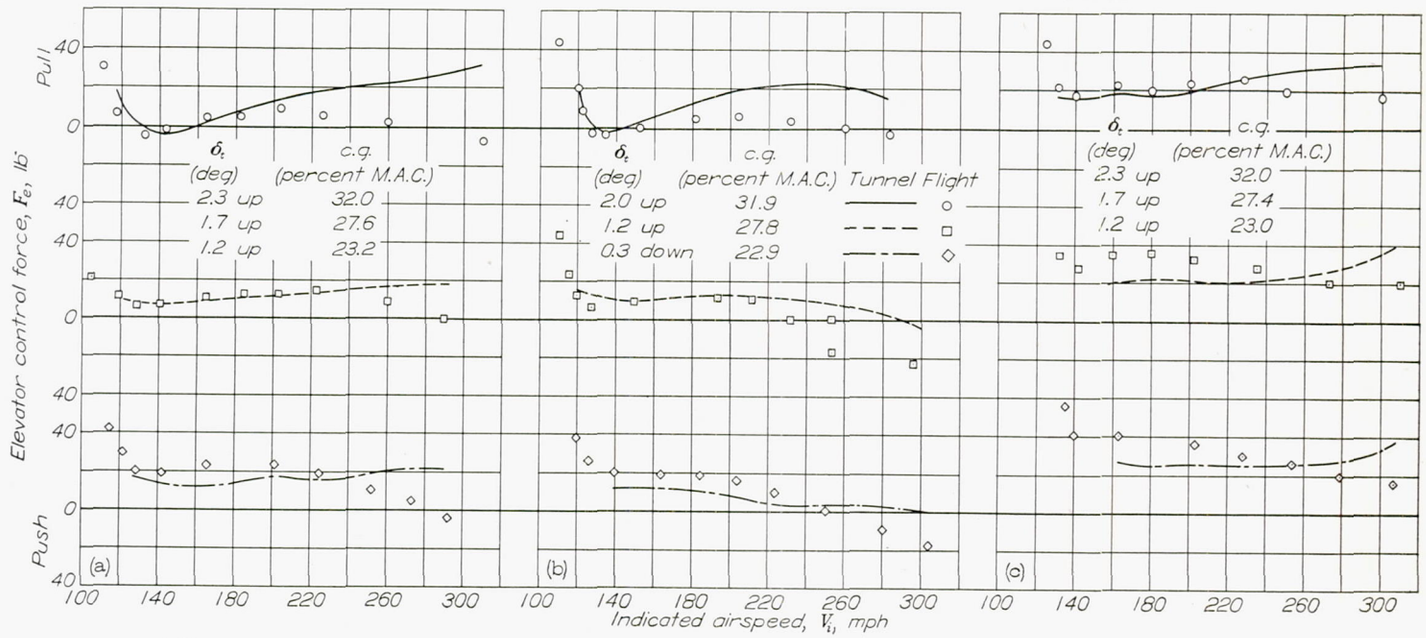

(a) Flaps retracted; rated power. (b) Flaps retracted; 75-percent rated power. (c) Flaps retracted; $T_c=0$.

FIGURE 11.—Variation of elevator control force with indicated airspeed. Model elevator and tab deflections identical with flight-test settings.

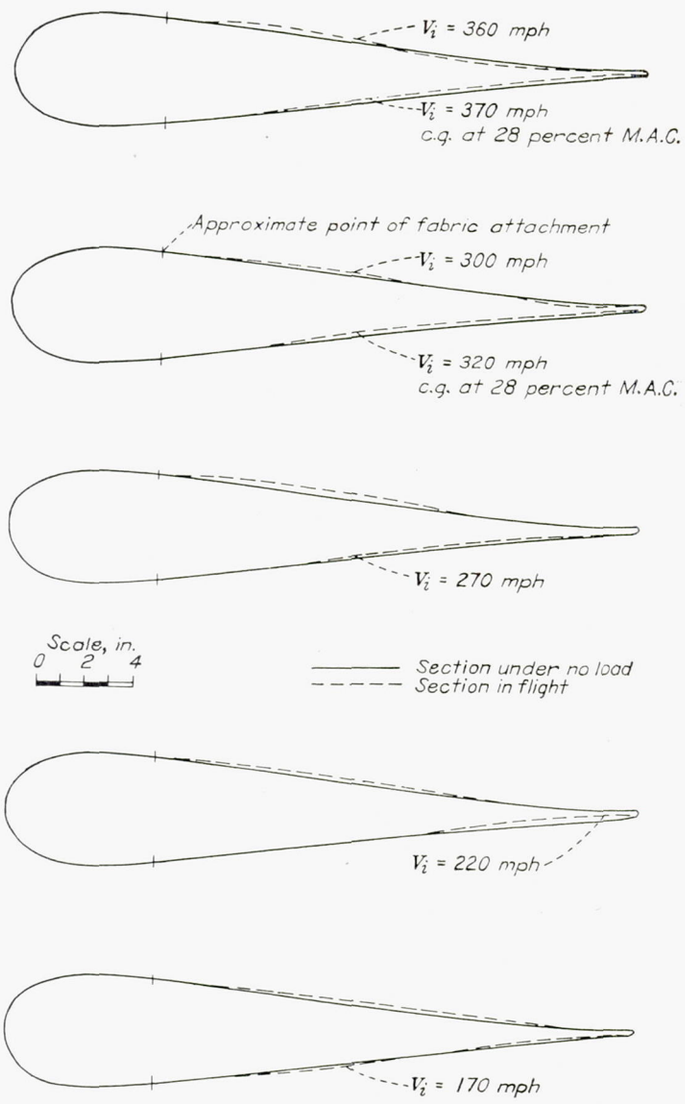

FIGURE 12.—Elevator-fabric distortion at various indicated airspeeds. No-load fabric tension, 2.7 pounds. Douglas A-26B airplane with center of gravity at 32 percent M.A.C. except where noted. Elevator section 84.2 inches from center line of airplane.

especially interesting to note the close agreement in the variation of aileron angle with sideslip, which serves as a flight-test indication of dihedral effect. It was found in the flight tests that the airplane wing in normal flight appeared to bend upward noticeably with respect to its position at rest. Despite the wing bending, however, the amount of effective dihedral determined from flight tests was also found to be no greater than that which would ordinarily be expected for an airplane of this type with 4.5° of geometric dihedral. Analysis of the elastic properties of the model wing under load indicates that the model wing bending was negligible. On the basis of the agreement between model and airplane results, it appears that the observed airplane wing bending may have had very little effect in increasing the dihedral effect beyond the normal amount for 4.5° of geometric dihedral. Further information regarding the elastic properties of the airplane wing and the effects of these properties would have been desirable but was not available. Comparison of the flight and tunnel aileron-force curves appears to indicate that little error was introduced in determination of the latter by the assumption that aileron hinge-moment characteristics remained unaffected by sideslip. The sideslip characteristics with flaps deflected do not agree so closely as do the flaps-retracted characteristics, particularly in the case of the aileron-deflection and rudder-force variations. The flight-test rudder forces show a tendency toward reversal in figure 14(c) but do not actually reverse as in the case of the model forces. At an airspeed slightly lower than that for which the data are presented, however, rudder-force reversal did appear in the flight tests in this wave-off condition. Dihedral effect with flaps deflected and rated power at low speed appears somewhat lower in the tunnel measurements than in the flight data. The flap deflection, however, was 5° greater on the model than on the airplane.

In figure 15, rudder hinge-moment characteristics estimated from flight-test rudder kicks are compared with rudder hinge-moment characteristics measured in the tunnel tests

with flaps retracted. Although the model rudder hinge-moment and force results are for an unsealed rudder and are also subject to effects of small surface and trailing-edge irregularities as in the case of the elevator results, agreement in this respect is good. As previously shown in figure 14, the rudder forces in steady sideslip are in good agreement for this flap condition. In regard to rudder hinge moments, the tunnel results, which showed no positive values of the parameter $\partial C_h/\partial\alpha$ for the rudder, indicated that no rudder snaking would occur in flight. This indication was confirmed in the flight tests.

Aileron characteristics.—No tunnel tests were made to investigate aileron characteristics for the 3:8 tab linkage with which the airplane was tested. If, however, linear tab effectiveness is assumed, these characteristics for the flaps-retracted condition can be estimated from the results of tunnel tests of the plain ailerons and the ailerons with a 1:1 balancing-tab ratio. Estimates of control force and helix

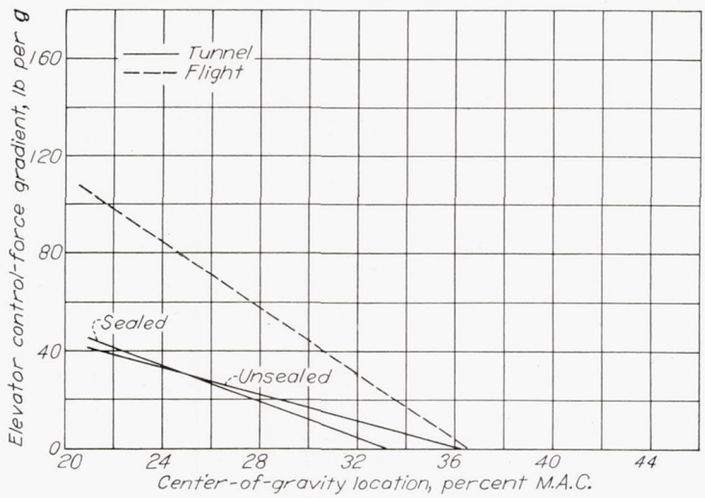

FIGURE 13.—Variation of elevator control-force gradient with center-of-gravity location estimated for sealed and unsealed elevators. V_i=260 miles per hour at 10,000-foot altitude; δ_f=0°; rated power; steady turning flight.

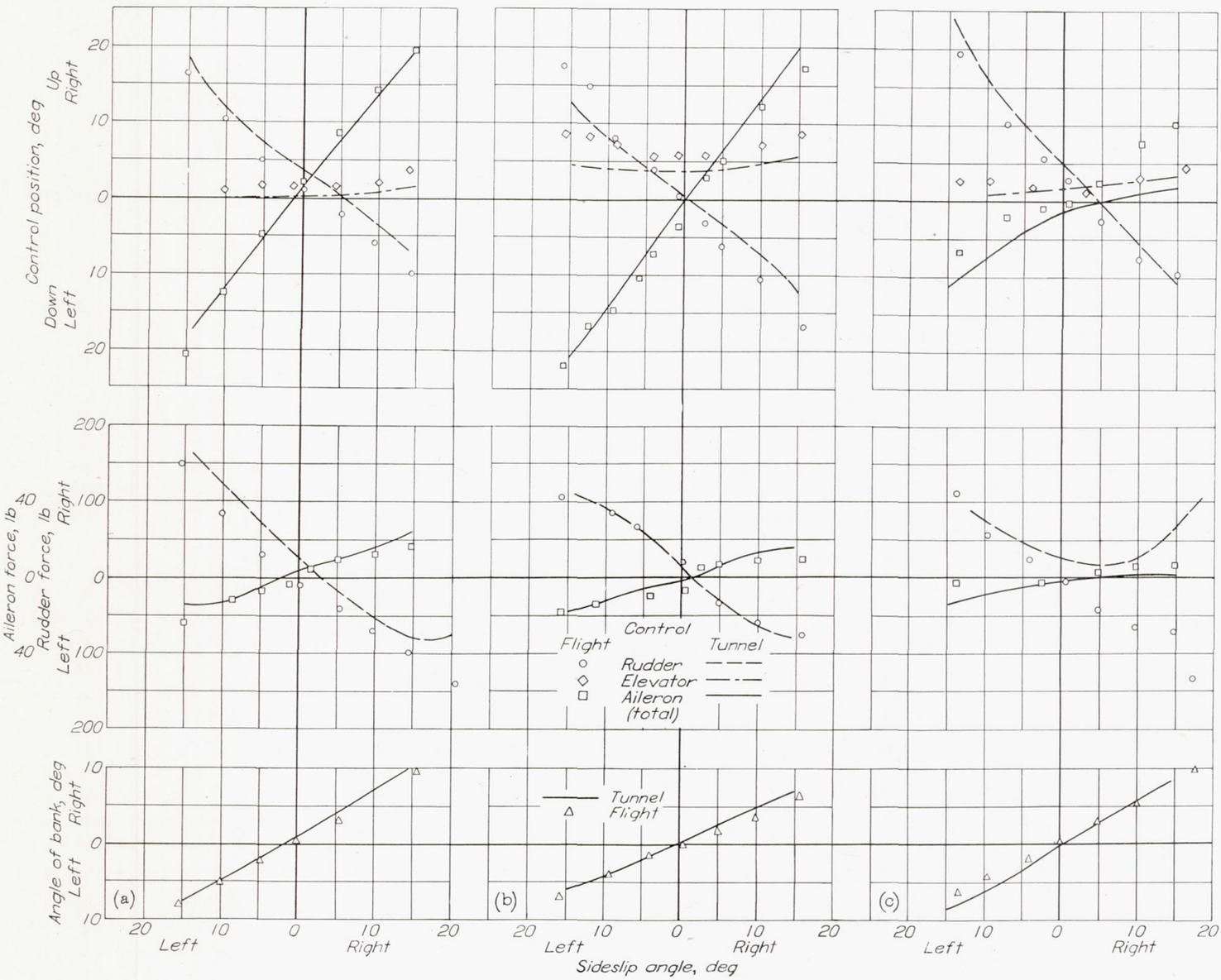

(a) Flaps retracted; rated power; V_i=141 miles per hour. (b) Flaps retracted; T_c=0; V_i=133 miles per hour. (c) Flaps deflected; rated power; V_i=111 miles per hour.

FIGURE 14.—Steady-sideslip characteristics.

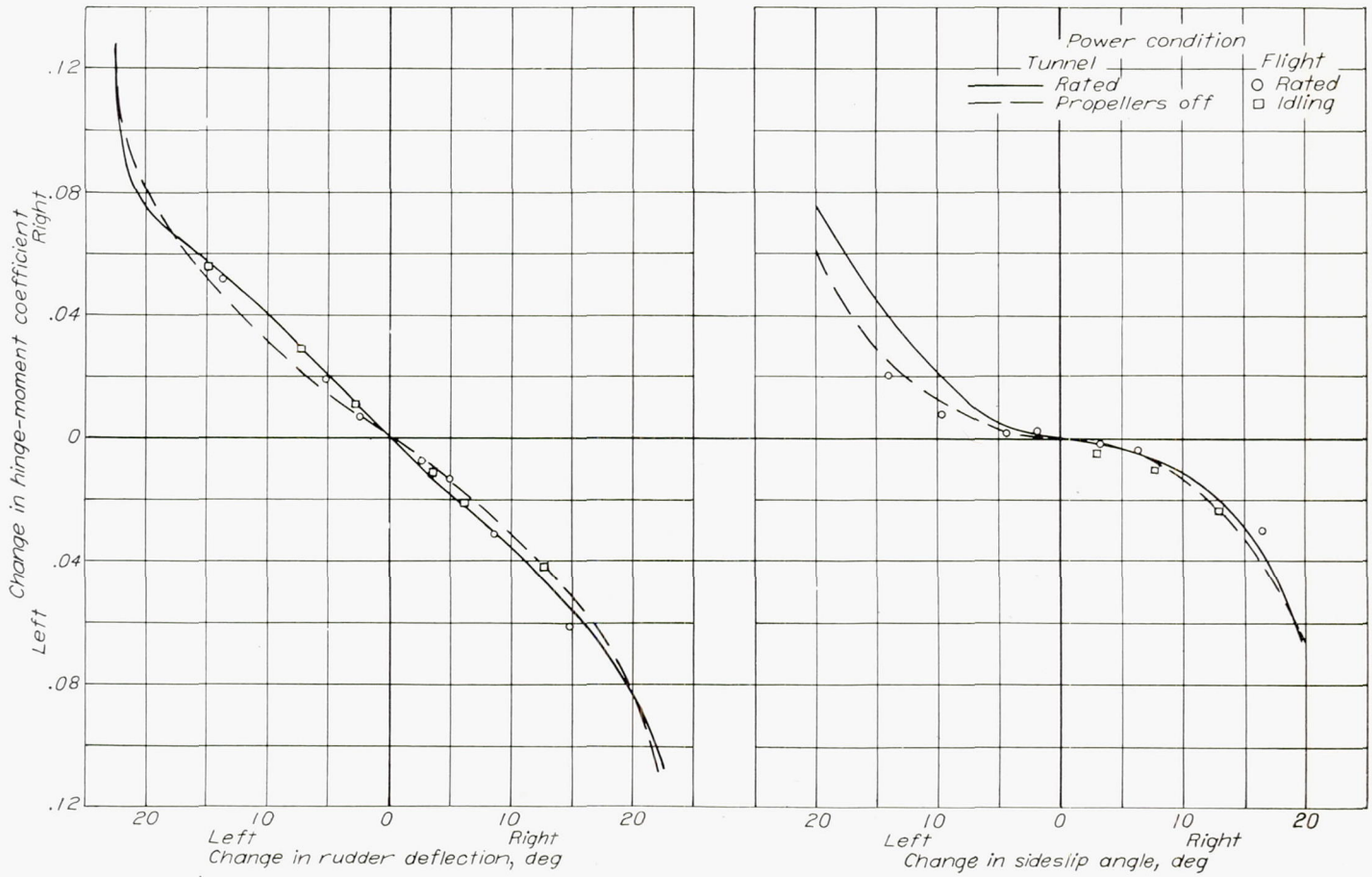

FIGURE 15.—Variation of rudder hinge-moment coefficient with rudder deflection and angle of sideslip at V_i=140 miles per hour. Flaps retracted.

angle made in this manner are compared with flight measurements in figure 16 for indicated airspeeds of 135 and 383 miles per hour. As recommended in reference 2, helix angles were estimated as $\frac{pb}{2V}=\frac{0.8C_l}{C_{l_p}}$, where C_l is the total aileron rolling-moment coefficient and a value of 0.57 was used as the damping-moment coefficient C_{l_p}. Although the angles of attack selected for these estimates correspond to rated-power flight at the appropriate speeds, the model aileron data were obtained in power-off static tests. Inasmuch as the tunnel measurements were made for right rolls only, the tunnel estimates are exactly symmetrical for right and left rolls, whereas the flight results are not. Agreement in the curves of helix angle is excellent in the range where comparison was possible. There is, however, some indication that the tunnel estimates, based on the arbitrary 0.8 factor, might be slightly optimistic for high deflections at high speed. At the low airspeed, agreement in the force curves is good except at the highest aileron deflections, where the control forces for given aileron deflections are slightly higher in the flight records than in the tunnel estimates. At the high speed, the control force required in flight for a total aileron deflection of 14° is approximately 40 pounds (or 38 percent) greater than the force indicated by the estimated curve. The greater discrepancies in the control forces at the high speed are believed largely due to the effects of aileron fabric distortion. As in the case of the elevator, the aileron fabric was found in the flight tests to undergo considerable distortion at this high speed. The distortion was in a direction to produce higher control forces.

If the assumption of linear tab effectiveness is not entirely valid, actual wind-tunnel tests with a 3:8 tab linkage would indicate the control forces somewhat lower than those estimated herein for the 3:8 linkage at the higher deflections.

Sideslip due to aileron deflection.—Curves of sideslip angle and rolling velocity against time in an abrupt rudder-fixed aileron roll out of a 30° banked turn are shown in figure 17. In addition to the simplified sideslip estimate of reference 2, the motions have been calculated by the operational method of reference 3 and also by the tabular-integration method of reference 4, in which slope variations in the curves of rolling-moment, yawing-moment, and side-force coefficients against angle of sideslip are taken into consideration. This method of tabular integration has been shown in reference 4 to be more reliable for general use than methods requiring the assumption of constant slopes.

For the subject airplane, which exhibited essentially constant slopes, the three methods of computation based on wind-tunnel results appear to give very similar results with respect to maximum sideslip angle, all of which are approximately 4° higher than the flight-test value. Among the factors possibly contributing to the lack of perfect agreement

is the difference between the instantaneous control deflection assumed for the computations and the actual control movement in the flight test. Another factor influencing the results may be the change in normal acceleration experienced by the airplane in its roll out of the turn. Although no flight record of normal acceleration was obtained for the test in question, similar flight-test results indicate that a considerable variation may have occurred during the maneuver. Analysis indicates that the change in normal acceleration and, consequently, lift coefficient may introduce conditions considerably different from those considered in the theoretical calculations.

A simple static estimate of the amount of rudder deflection required to maintain zero sideslip in an aileron roll was made as suggested in reference 2; that is, it was assumed that the desired rudder deflection would be that required to counteract the combination of aileron adverse yawing moment and yawing moment due to rolling. The estimated value obtained by this method was approximately 8° for flaps-retracted flight with level-flight power at an indicated airspeed of 145 miles per hour. Although no flight-test data were recorded for full-aileron rolls at this flight condition in which zero sideslip was maintained by means of varying rudder deflections, flight-test records for constant rudder settings indicate that the rudder deflection estimated from tunnel results would be noticeably lower than that required in flight. For several rolls with partly deflected ailerons, however, essentially zero sideslip was maintained, and the estimated rudder deflections were found to be in fair agreement with the maximum deflections required in flight.

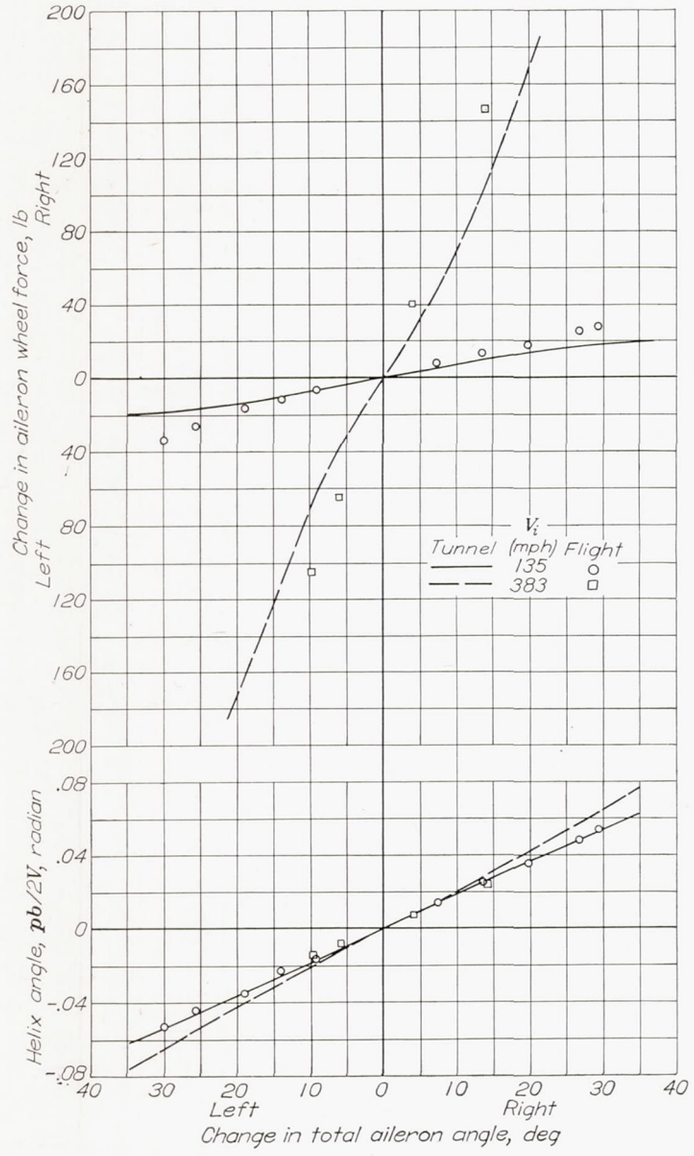

FIGURE 16.—Variation of aileron wheel force and helix angle $pb/2V$ with change in total aileron angle in rolls with rudder fixed, flaps retracted, and rated power.

CONCLUDING REMARKS

Stability and control characteristics determined from Langley 19-foot-pressure-tunnel tests of a 0.2375-scale powered model of the Douglas XA–26 airplane have been compared with results of flight tests of a Douglas A–26B airplane.

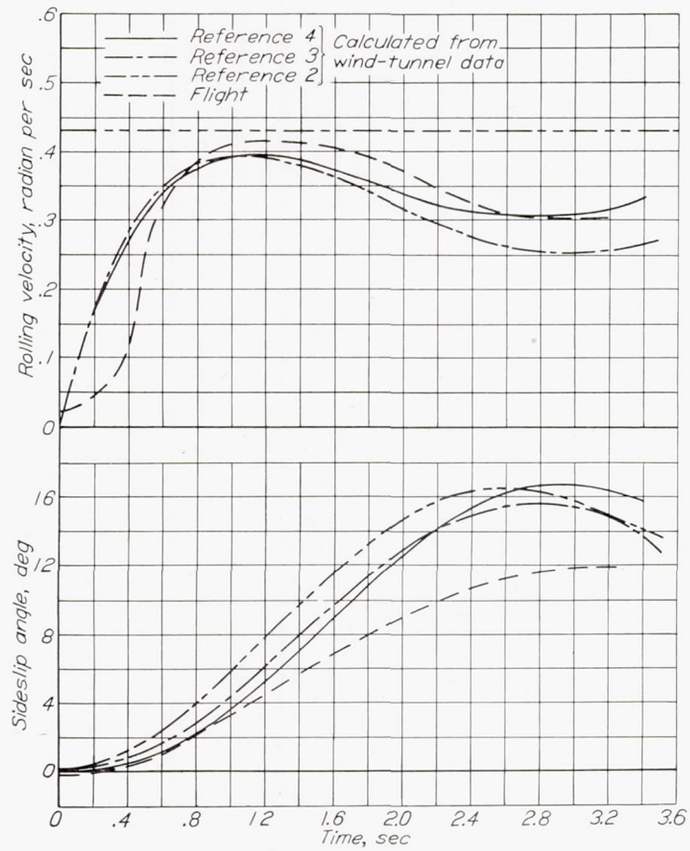

FIGURE 17.—Rolling velocity and sideslip angle during aileron roll out of 30° banked turn. $\delta_f=0°$; $V_i=145$ miles per hour at 10,000-foot altitude; level-flight power.

The significant results of the comparison may be summarized as follows:

1. Good correlation was obtained regarding elevator-fixed neutral points and the variation of elevator deflection in both straight and turning flight except at speeds approaching the stall. At these low speeds the airplane showed a distinct improvement in stability not indicated by the model tests. The difference was attributed to the fact that the pronounced stalling at the root of the production airplane wing did not take place on the smooth, well-faired model wing.

2. The variations of elevator control force with airspeed and acceleration were not in good agreement. Although some discrepancy was introduced by the absence of a seal on the model elevator and by small differences in absolute values of elevator deflection, the correlation in control-force characteristics was also influenced by the effects of fabric distortion at high speeds and by small construction dissimilarities such as differences in trailing-edge angle.

3. Elevator tab effectiveness as determined from tunnel data was in good agreement with flight-test tab effectiveness.

4. Agreement in both rudder-fixed and rudder-free static directional stability was good except in the wave-off condition, in which the model tests indicated rudder-force reversal at a higher speed than the flight tests.

5. Model and airplane indications of stick-fixed and stick-free dihedral effect were in good agreement, although some slight difference in geometric dihedral may have existed because of wing bending in flight. The use of model hinge-moment data obtained at zero sideslip appeared to be satisfactory for the determination of aileron forces in sideslip.

6. Fairly good correlation in aileron effectiveness and control forces was obtained. Fabric distortion was believed responsible to some extent for higher flight values of aileron force at high speeds.

7. Estimation of sideslip developed in an abrupt aileron roll was fair, but determination of the maximum rudder deflection required to maintain zero sideslip in an abrupt roll was not entirely satisfactory.

On the basis of these findings, it appears that agreement between stability and control characteristics estimated from wind-tunnel results and those measured in flight cannot be completely satisfactory unless certain factors now usually neglected in wind-tunnel testing can be taken into consideration. These factors involve small differences between the model and the airplane and include differences in elastic properties, surface finish, and construction accuracy. These factors should be considered, if possible, in future investigations.

LANGLEY MEMORIAL AERONAUTICAL LABORATORY,
NATIONAL ADVISORY COMMITTEE FOR AERONAUTICS,
LANGLEY FIELD, VA., *August 11, 1945.*

REFERENCES

1. Mathews, Charles W.: An Analytical Investigation of the Effects of Elevator-Fabric Distortion on the Longitudinal Stability and Control of an Airplane. NACA ACR No. L4E30, 1944.
2. Kayten, Gerald G.: Analysis of Wind-Tunnel Stability and Control Tests in Terms of Flying Qualities of Full-Scale Airplanes. NACA Rep. No. 825, 1945.
3. Jones, Robert T.: A Simplified Application of the Method of Operators to the Calculation of Disturbed Motions of an Airplane. NACA Rep. No. 560, 1936.
4. Wolowicz, Chester H.: Prediction of Motions of an Airplane Resulting from Abrupt Movement of Lateral or Directional Controls. NACA ARR No. L5E02, 1945.

U. S. GOVERNMENT PRINTING OFFICE: 1948

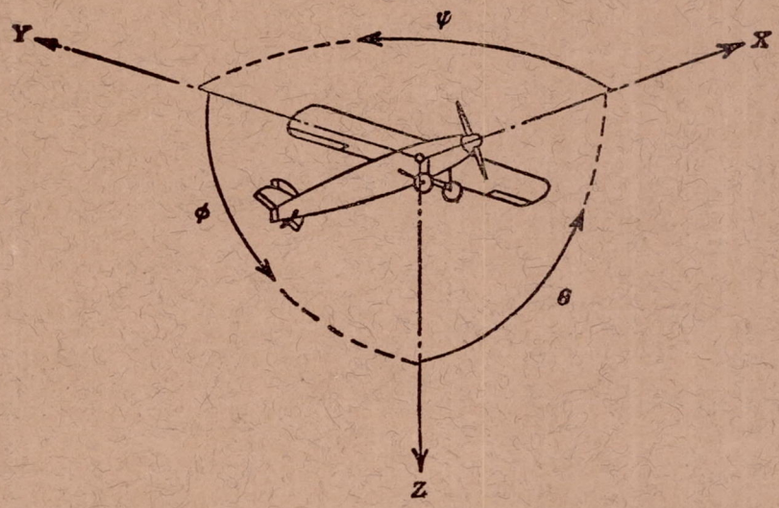

Positive directions of axes and angles (forces and moments) are shown by arrows

Axis		Force (parallel to axis) symbol	Moment about axis			Angle		Velocities	
Designation	Symbol		Designation	Symbol	Positive direction	Designation	Symbol	Linear (component along axis)	Angular
Longitudinal	X	X	Rolling	L	$Y \longrightarrow Z$	Roll	ϕ	u	p
Lateral	Y	Y	Pitching	M	$Z \longrightarrow X$	Pitch	θ	v	q
Normal	Z	Z	Yawing	N	$X \longrightarrow Y$	Yaw	ψ	w	r

Absolute coefficients of moment

$C_l = \frac{L}{qbS}$ (rolling) $\quad C_m = \frac{M}{qcS}$ (pitching) $\quad C_n = \frac{N}{qbS}$ (yawing)

Angle of set of control surface (relative to neutral position), δ. (Indicate surface by proper subscript.)

4. PROPELLER SYMBOLS

D Diameter

p Geometric pitch

p/D Pitch ratio

V' Inflow velocity

V_s Slipstream velocity

T Thrust, absolute coefficient $C_T = \frac{T}{\rho n^2 D^4}$

Q Torque, absolute coefficient $C_Q = \frac{Q}{\rho n^2 D^5}$

P Power, absolute coefficient $C_P = \frac{P}{\rho n^3 D^5}$

C_s Speed-power coefficient $= \sqrt[5]{\frac{\rho V^5}{P n^2}}$

η Efficiency

n Revolutions per second, rps

Φ Effective helix angle $= \tan^{-1}\left(\frac{V}{2\pi r n}\right)$

5. NUMERICAL RELATIONS

1 hp=76.04 kg-m/s=550 ft-lb/sec

1 metric horsepower=0.9863 hp

1 mph=0.4470 mps

1 mps=2.2369 mph

1 lb=0.4536 kg

1 kg=2.2046 lb

1 mi=1,609.35 m=5,280 ft

1 m=3.2808 ft